A novel sample handling system for dissolution dynamic nuclear polarization experiments

Thomas Kress[1], Kateryna Che[2], Ludovica M. Epasto[2], Fanny Kozak,[2] Gregory L. Olsen[2], Albina Selimovic[2], Dennis Kurzbach[2,*]

[1] Department of Chemistry, University of Cambridge, Lensfield Road, Cambridge CB2 1EW, UK.

[2] University Vienna, Faculty of Chemistry, Institute of Biological Chemistry, Währinger Str. 38, Vienna, Austria.

* Corresponding author. E-Mail: dennis.kurzbach@univie.ac.at

Abstract

We present a system for facilitated sample vitrification, melting, and transfer in dissolution dynamic nuclear polarization (DDNP) experiments. For DDNP, a sample is typically hyperpolarized at cryogenic temperatures before dissolution with hot solvent and transfer to a nuclear magnetic resonance (NMR) spectrometer for detection in the liquid state. The resulting signal enhancements can exceed four orders of magnitude. However, the sudden temperature jump from cryogenic temperatures close to 1 K to ambient conditions imposes a particular challenge. It is necessary to rapidly melt the sample to avoid a prohibitively fast decay of hyperpolarization. Here, we demonstrate a sample dissolution method that facilitates the temperature jump by eliminating the need to open the cryostat used to cool the sample. This is achieved by inserting the sample through an airlock in combination with a dedicated dissolution system that is inserted through the same airlock shortly before the melting event. The advantages are threefold: 1. The cryostat can be operated continuously at low temperatures. 2. The melting process is rapid as no pressurization steps of the cryostat are required. 3. Blockages of the dissolution system due to freezing of solvents during melting and transfer are minimized.

Dedicated to Prof. Geoffrey Bodenhausen on the occasion of his 70th Birthday.

Introduction

Dissolution dynamic nuclear polarization (DDNP) (Ardenkjaer-Larsen, Fridlund et al. 2003, Kovtunov, Pokochueva et al. 2018, Jannin, Dumez et al. 2019) is a method used for hyperpolarizing nuclear spins at cryogenic temperatures (Abragam and Goldman 1978) close to 1 K - typically attained in a liquid helium-cooled cryostat at low pressures - coupled to subsequent temperature jump and detection at ambient conditions in a conventional liquid-state nuclear magnetic resonance (NMR) spectrometer. Spin hyperpolarization is here understood as the constructive alignment of large shares of nuclear spins parallel or antiparallel to a magnetic field B_0. The transfer of the hyperpolarized sample from DNP conditions at low temperatures to NMR conditions at ambient temperature is typically achieved with a burst of hot solvent. It rapidly dissolves the sample and pushes it through a capillary to the detection spectrometer. One can thus achieve signal enhancements in liquid state NMR of four orders of magnitude. (Vuichoud, Milani et al. 2015) Capitalizing on the resulting improved sensitivity, DDNP has found various applications in recent years, including real-time metabolomics (Liu and Hilty 2018, Sadet, Emmanuelle M. M. Weber et al. 2018), reaction monitoring (Boeg, Duus et al. 2019), structural biology (Szekely, Olsen et al. 2018, Wang and Hilty 2019), and detection of long-lived spin states (Tayler, Marco-Rius et al. 2012, Bornet, Ji et al. 2014). However, DDNP instrumentation is still actively being developed to improve its cost-efficiency and reliability, and a need for user-friendly DDNP systems persists.

The sample insertion into and dissolution from the cryostat poses a challenge in designing such systems as both events introduce large heat quantities and warm the instrumentation. The heat shock needs to be compensated by the liquid helium bath within the cryostat (Ardenkjaer-Larsen, Bowen et al. 2019) at the expense of prolonged experimental polarization times or polarization losses. Besides, if the temperature of the capillaries used for transfer drops excessively after insertion, the liquid used to dissolve the sample may freeze before exiting the cryostat, preventing the liquid containing the hyperpolarized substance from reaching the NMR spectrometer for detection.

Two widely used solutions to these problems have been proposed:

1   1. To minimize the heat-load Ardenkjaer-Larsen and co-workers have developed a sample insertion and
2   dissolution system based on a 'fluid path' and a 'dynamic seal' as proposed in their original design for the SpinLab
3   DDNP system. (Malinowski, Lipso et al. 2016) The capillaries guiding the dissolution solvent are slowly inserted
4   into the cryostat together with the sample through an airlock. Thus, one can put the capillaries and sample in
5   place without breaking the cryostat's vacuum. After the DNP procedure, the sample can be dissolved through
6   the already positioned capillaries. However, as these are also held at cryogenic temperatures during the DNP
7   build-up period, the dissolution solvent might freeze if the joints between the sample holder and solvent
8   inlet/outlet are not carefully sealed to avoid liquid helium entering the sample chamber.

9   2. Alternatively, in a second approach inspired by the original 'HyperSense' apparatus, the cryostat is pressurized
10 with helium gas and opened briefly to insert the sample. Bodenhausen and co-workers successfully adapted this
11 design to recently developed DDNP systems. (Kurzbach, Weber et al. 2016, Baudin, Vuichoud et al. 2018) After
12 completing the DNP procedure, the cryostat is pressurized and opened again to insert the capillaries needed for
13 the dissolution event. This design has the advantage of minimizing the risk of freezing the dissolution solvent as
14 the capillaries are not cooled down during the DNP period. However, this comes at the expense of increased heat
15 exchange and helium losses during sample insertion and dissolution compared to the fluid-path design.
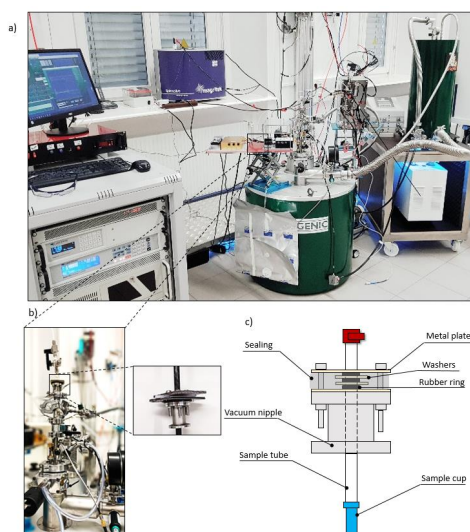
16

17 **Figure 1.** a) The cryogen-consumption-free DDNP system (green magnet) used together with the proposed hybrid sample handling system.
18 The low-field spectrometer (blue magnet) used here for detection is situated in the back. b) Zoom on the airlock atop the DDNP system with
19 the vacuum seal attached. The smaller panel shows the detached seal. c) Scheme of the seal (grey), the sample chamber (blue), and the
20 sample tube (white). An array of washers, a silicon fitting, and O-rings renders the seal vacuum-tight, while the sample stick can be moved
21 vertically. The seal is attached to the airlock atop the DNP system via a vacuum nipple. (Images by K. Che and L. M. Epasto.)

22 To capitalize on both systems' advantages, namely the efficiency of the 'fluid path' and the robustness of
23 dissolution experiments in pressurized systems, we have developed a hybrid sample handling design. Here, the
24 sample is inserted through an airlock and a vacuum seal system that enables insertion with minimal heat load,
25 while at the same time, sample dissolution can be performed with warm capillaries and without breaking the
26 cryostat's vacuum.

27 We here demonstrate this design's implementation in a cryogen consumption-free DNP system operating at 6.7
28 T and a base temperature of 1.3 K.

29 **Results and Discussion**

30 The proposed sample handling device is described in Fig. 1. The entire DNP system and the spectrometer used
31 for liquid-state detection are shown in Fig. 1a. The most crucial component of the sample handling system is a
32 vacuum seal that surrounds a hollow carbon fiber rod, which we denote as 'sample tube'. The seal is placed atop
33 an airlock via a vacuum nipple (Fig. 1b). The seal itself is closed vacuum-tightly around the sample tube via

1   alternating layers of washers and O-rings pressed together by two metal plates (Fig. 1c). A lateral rubber sealing
2   additionally encloses the seal.

3
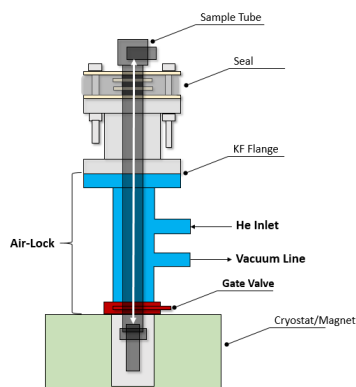
Figure 2. Scheme of the airlock system (blue/red) situated between the seal and the cryostat. The latter can be sealed with a gate valve. The
sample tube can be inserted upon opening the gate valve. With the He inlet and the connection to a vacuum line, air can be purged from the
airlock. The double-headed white arrow indicates the sample tube sliding path through the seal and the airlock into and out of the cryostat
(Figure not to scale.)

8   When mounted on top of the cryostat, the combination of airlock and vacuum-seal allows one to slide the sample
9   tube relative to the seal and position it inside the cryostat without the need to open the latter or break the
10   vacuum within (cf. Fig. 2). A sample can thus be inserted without opening the DNP system to the atmosphere,
11   thereby preventing air from condensing in the cryostat.

12   The sample tube is closed at its lower end by a 'sample cup' containing the substance to be hyperpolarized, and
13   at its top by a ball valve (Fig. 3a). Hence, it constitutes a closed volume inserted into the cryostat after being
14   flushed with helium gas. The top-end remains at room temperature above the vacuum seal (outside the cryostat),
15   while the sample cup is pushed into the cryostat until it reaches the liquid helium bath where the sample is
16   hyperpolarized.

17   Once hyperpolarized, the sample can be dissolved by opening the ball valve and inserting a 'dissolution stick' that
18   is connected via a PTFE capillary to a pressure heater that provides the hot solvent (here 5 mL of D_2O at a pressure
19   of 1.5 MPa and a temperature of 513 K) used for dissolution. Fig. 3a and b show how the dissolution stick inserts
20   into the sample tube and the cup containing the hyperpolarized substance. The inbound and outbound fluid
21   paths are inserted with the dissolution stick such that both are at ambient temperature during the process. Upon
22   insertion of the dissolution stick, the superheated D_2O is squirted onto the sample via the dissolution stick's inner
23   capillary (Fig. 3b), dissolving it and pushing it out of the cryostat. The dissolved sample is ejected through the
24   lumen between the inner capillary and the outer tube.

25
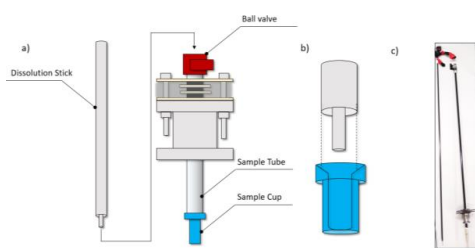
Figure 3. a) Scheme of the dissolution system (airlock and polarizer omitted for clarity). For a dissolution, the ball valve (red) on top of the
sample tube is opened. The sample cup is lifted 100 mm above the liquid helium bath at the bottom of the cryostat. The dissolution stick is
then inserted. b) Sketch of how the dissolution stick consisting of two coaxial capillaries (grey) is inserted into the sample cup (blue). The hot
solvent is squirted onto the sample through the inner capillary—the lumen between the inner and outer capillary forms the liquid-outlet. c)
Image of the sample stick (left) and sample tube (right) with the seal and sample cup attached. (Image by L. M. Epasto.)

31   Fig. 4 displays the path the solvent takes upon dissolution. After melting of the hyperpolarized sample,
32   pressurized helium gas propels the hyperpolarized liquid from the outlet at the top end of the dissolution stick

1 to an NMR tube waiting in a spectrometer for detection. The capillary connecting the DNP and detection
2 spectrometers is surrounded by a copper solenoid that provides a 37 mT magnetic field, as originally devised by
3 Meier and co-workers in the context of so-called 'bullet DNP' (Kouřil, Kouřilová et al. 2018). The solenoid
4 effectively shields the transfer path from low magnetic fields that can prohibitively accelerate the relaxation of
5 hyperpolarization. Similar approaches based on 'magnetic tunnels' using permanent magnets have also been
6 successful. (Milani, Vuichoud et al. 2015)
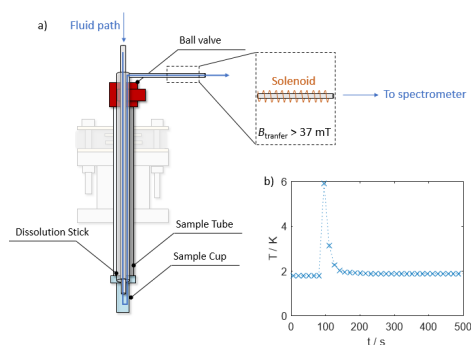
7

8 **Figure 4**. a) Scheme of sample tube with dissolution stick inserted. The inlet for the hot D_2O and the path the fluid takes is marked with a
9 blue arrow. The outlet capillary exiting towards the detection spectrometer is surrounded by a solenoid to maintain a constant magnetic
10 field during the sample transfer. Note that the magnetic field within the solenoid is perpendicular to the field of the DNP apparatus and the
11 detection spectrometer. b) Temperature profile during a dissolution experiment. During the dissolution, the temperature rises by 4 K and
12 subsequently returns to stand-by temperature within a minute.

13 Upon completing the experiment, the sample tube and dissolution stick are removed from the cryostat by sliding
14 both upward through the vacuum seal until the airlock can be closed. Fig. 4b displays the temperature changes
15 observed within the cryostat during the dissolution event and demonstrates the relatively low heat-load.

16 Fig. 5 displays hyperpolarized HDO spectra obtained with the proposed system using a sample containing 40 mM
17 TEMPOL in a mixture of 50% glycerol-d_8, 40% D_2O, and 10% H_2O. In this example, a series of 1D NMR signals was
18 detected at one-second intervals on a benchtop spectrometer operating at B_0 = 1 T, using a 10° flip angle pulse.
19 The resulting ^{1}H signal enhancement was ε ≈ 36 000, corresponding to a polarization of P (^{1}H) ≈ 12%. In the solid-
20 state, a polarization of P (^{1}H) = 15 ± 3% was achieved at 1.8 K, indicating that ca. 25% of the proton
21 hyperpolarization was lost during the transfer. In contrast, when the solenoid was removed, P (^{1}H) of only ca. 7%
22 was observed, corresponding to a significantly larger ca. 57% polarization loss. Fig. 5a shows how the signal
23 intensity decays after injection into the benchtop NMR spectrometer. Fig. 5b shows the first detected signal
24 immediately after injection overlaid upon the corresponding thermal equilibrium signal detected with the same
25 pulse angle. Fig. 5c shows the decay of the signal enhancement at a 1 s sampling interval. The hyperpolarization
26 decays to naught exponentially with a relaxation rate of R_1 = 0.14 ± 0.1 s^{-1}. Polarization levels obtained using the
27 hybrid system presented here are competitive with those previously reported for other dissolution systems. For
28 example, Vuichoud et al. (Vuichoud, Bornet et al. 2016) reported 6% and Ardenkjear-Larsen et al. (Lipso, Bowen
29 et al. 2017) 13% [1]H water polarizations with comparable samples derived from TEMPOL/water-glycerol mixtures.
30 (Leavesley, Wilson et al. 2018) Furthermore, the hybrid system is fully compatible with recent polarization
31 approaches capable of providing polarization levels of up to 70%, obtained using samples containing UV-induced
32 radicals. (Pinon, Capozzi et al. 2020)
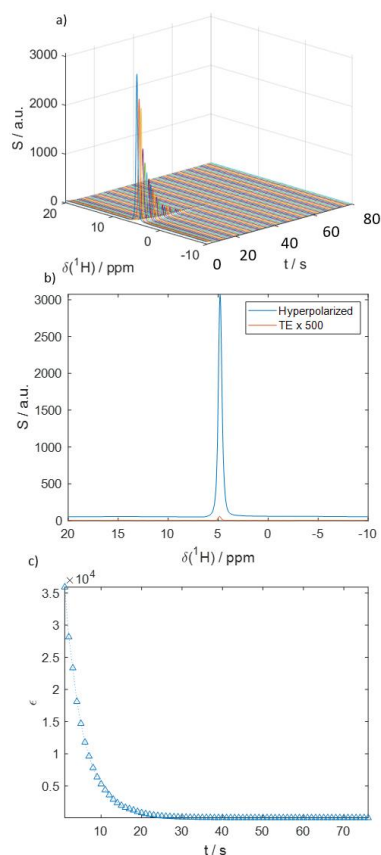
Figure 5. a) Time series of ^{1}H-detected spectra of hyperpolarized HDO at B_0 = 1 T. At t = 0 the hyperpolarized liquid is injected into the spectrometer. The transfer took ca. 1 s over a length of 1.5 m. b) The HDO spectrum directly after injection (blue) compared to the signal in thermal equilibrium (orange). The signal enhancement was ε ≈ 36 000, corresponding to a ^{1}H polarization of P (^{1}H) ≈ 12 %. The detection flip angle was α = 10°. c) Decay of the signal enhancement in comparison to thermal equilibrium with time after injection. The mono-exponential decay rate constant R_1 was fitted to 0.21 +/- 0.03 s^{-1}.

Conclusions

The proposed sample handling system for dissolution DNP has three advantages: 1. The cryostat can be maintained at low temperatures, and the vacuum within is not broken at any stage of the dissolution process. In addition, the heat-load introduced during dissolution is reduced as the dissolution stick does not come into contact with the helium bath. 2. The melting process is very rapid as pressurization of the cryostat is eliminated, in contrast to other HyperSense-inspired systems. 3. Freezing and blockage of the dissolution system are avoided as the dissolution stick is not cooled down at any stage of the experiment.

The system is furthermore readily adaptable to different polarizer systems as the vacuum nipple connecting the seal to the DNP apparatus can be adjusted to any flange size. The system is also compatible with narrow sample spaces. For example, the sample tube needs to pass through a bore as narrow as 12 mm in the system presented here.

In conclusion, using this compact and cost-efficient sample handling system, it is possible to perform dissolution DNP experiments with a cryogen consumption-free cryostat without risking quenching of the magnet or introducing air contamination into the cryostat. Moreover, following dissolution, the system reliably returns to its stand-by temperature within a minute, which is a promising step towards higher throughput DDNP.

Experimental

MAGNETIC
RESONANCE
Open Access
Discussions

1   For DNP 50 μL of a solution of 40 mM TEMPOL in a mixture of 50% glycerol-d_8, 40% D_2O, and 10% H_2O was
2   hyperpolarized at 1.8 K in a magnetic field of 6.7 T for 2500 s using continuous-wave microwave irradiation at
3   188.08 GHz. DNP samples were always freshly prepared to avoid ripening effects. (Weber, Sicoli et al. 2018) Fig.
4   6 displays the build-up kinetics. A VDI microwave source was used together with a 16x frequency multiplier that
5   provided an output power for the microwave of ca. 50 mW. The magnet-cryostat combination was purchased
6   from Cryogenic Ltd. and operated as described in reference (Baudin, Vuichoud et al. 2018).

7   For detection of the solid-state polarization, a 400 MHz Bruker Avance III system was adapted to a ^{1}H resonance
8   frequency of 285.3 MHz by using a broad-band preamplifier for the proton channel. The detection circuit and the
9   external tune-and-match system were home-built, as described in reference (Baudin, Vuichoud et al. 2018). To
10   monitor the build-up, detection pulses with a flip angle of 1 degree were applied every 5 s.
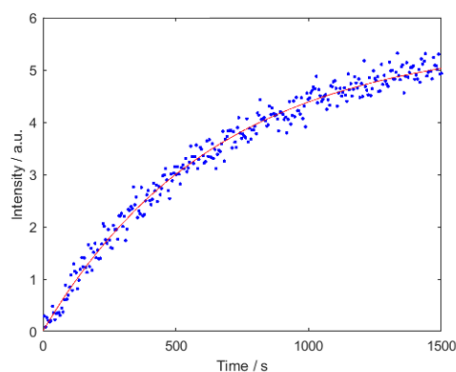
11

12   **Figure 6.** Polarization build-up curve at 1.8 K. The build-up rate constant was 0.0016 +/- 0.0001 s^{-1}. The polarization was of P (^{1}H) ≈ 15 ±- 2%.

13   After DNP, the sample was dissolved with a burst of 5 mL D_2O at 1.5 MPa as described in the main text. The
14   hyperpolarized liquid was then pushed with helium gas at 0.7 MPa to the detection spectrometer. The dissolution
15   process employed a home-built pressure heater actuated with an Arduino micro-controller. A home-written
16   MATLAB-based user interface controls the dissolution and injection steps. The hyperpolarized liquid was
17   transferred to a Magritek SpinSolve Phosphorous spectrometer operating at room temperature and a magnetic
18   field of 1 T. The transfer path was ca. 1.5 m long and the transfer took ca. 1 s. A PTFE capillary with a 1 mm inner
19   diameter and 3.2 mm outer diameter was used. The solenoid (2 turns / mm) surrounding the transfer path
20   provided a 37 mT magnetic field during the sample transfer at a current of 3 A and a power of 450 W. The
21   solenoid ended ca. 500 mm before reaching the bore of the magnet. To avoid heating of the PTFE capillary path,
22   the solenoid was only switched on during the transfer.

23   A volume of 600 μL of the hyperpolarized liquid was directly injected into an NMR tube that was treated with
24   strongly oxidizing rinsing solutions (Helmanex III) beforehand to reduce the likelihood of gas inclusions forming
25   upon injection into the NMR tube and disrupting NMR detection. (Dey, Charrier et al. 2020)

26   In the liquid state, ^{1}H single pulse acquisitions were repeated at one-second intervals, using a flip angle of 10
27   degrees. The spectral width was 30 ppm at a carrier frequency centered at 5 ppm. The spectrometer's external
28   lock system was used for referencing the chemical shift.

29   All data were processed with home-written scripts using the MATLAB 2019 software package. All data were zero-
30   filled and apodized with a Gaussian window function before Fourier transformation.

31   **Acknowledgments**

MAGNETIC RESONANCE
Open Access Discussions

3 **Author contribution**

4 TK, KC, LME, FK, GO, AS and DK built the DDNP system and performed experiments. DK wrote the manuscript
5 with the help of all authors.

6 **Competing interest**

7 The authors declare no conflict of interest.

8 **Data availability**

9 All data are available from the authors upon request.

10 **References**

11 Abragam, A. and M. Goldman (1978). "Principles of Dynamic Nuclear-Polarization." Reports on
12 Progress in Physics **41** (3): 395-467.

13 Ardenkjaer-Larsen, J. H., S. Bowen, J. R. Petersen, O. Rybalko, M. S. Vinding, M. Ullisch and N. C.
14 Nielsen (2019). "Cryogen-free dissolution dynamic nuclear polarization polarizer operating at 3.35 T,
15 6.70 T, and 10.1 T." Magn Reson Med **81** (3): 2184-2194.

16 Ardenkjaer-Larsen, J. H., B. Fridlund, A. Gram, G. Hansson, L. Hansson, M. H. Lerche, R. Servin, M.
17 Thaning and K. Golman (2003). "Increase in signal-to-noise ratio of > 10,000 times in liquid-state NMR."
18 Proc Natl Acad Sci U S A **100** (18): 10158-10163.

19 Baudin, M., B. Vuichoud, A. Bornet, J. Milani, G. Bodenhausen and S. jannin (2018). "A Cryogen-
20 Free 9.4 T System for Dynamic Nuclear Polarization." J. Magn. Reson., **294**: 115-121.

21 Boeg, P. A., J. Ø. Duus, J. H. Ardenkjær-Larsen, M. Karlsson and S. Mossin (2019). "Real-Time
22 Detection of Intermediates in Rhodium-Catalyzed Hydrogenation of Alkynes and Alkenes by
23 Dissolution DNP." J. Chem. Phys. C **123**: 9949-9956.

24 Bornet, A., X. Ji, D. Mammoli, B. Vuichoud, J. Milani, G. Bodenhausen and S. Jannin (2014). "Long-
25 Lived States of Magnetically Equivalent Spins Populated by Dissolution-DNP and Revealed by Enzymatic
26 Reactions." Chemistry-a European Journal **20** (51): 17113-17118.

27 Dey, A., B. Charrier, E. Martineau, C. Deborde, E. Gandriau, A. Moing, D. Jacob, D. Eshchenko, M.
28 Schnell, R. Melzi, D. Kurzbach, M. Ceillier, Q. Chappuis, S. F. Cousin, J. G. Kempf, S. Jannin, J. N. Dumez
29 and P. Giraudeau (2020). "Hyperpolarized NMR Metabolomics at Natural (13)C Abundance." Anal
30 Chem **92** (22): 14867-14871.

31 Jannin, S., J. N. Dumez, P. Giraudeau and D. Kurzbach (2019). "Application and methodology of
32 dissolution dynamic nuclear polarization in physical, chemical and biological contexts." J Magn Reson
33 **305**: 41-50.

34 Kouřil, K., H. Kouřilová, M. H. Levitt and B. Meier (2018). "Dissolution-Dynamic Nuclear Polarization
35 with Rapid Transfer of a Polarized Solid." arXiv:1807.00223 [physics.ins-det].

36 Kovtunov, K. V., E. V. Pokochueva, O. G. Salnikov, S. F. Cousin, D. Kurzbach, B. Vuichoud, S. Jannin,
37 E. Y. Chekmenev, B. M. Goodson, D. A. Barskiy and I. V. Koptyug (2018). "Hyperpolarized NMR
38 Spectroscopy: d-DNP, PHIP, and SABRE Techniques." Chem Asian J.

1   Kurzbach, D., E. M. M. Weber, A. Jhajharia, S. F. Cousin, A. Sadet, S. Marhabaie, E. Canet, N.
2   Birlirakis, J. Milani, S. Jannin, D. Eshchenko, A. Hassan, R. Melzi, S. Luetolf, M. Sacher, M. Rossire, J.
3   Kempf, J. A. B. Lohman, M. Weller, G. Bodenhausen and D. Abergel (2016). "Dissolution Dynamic
4   Nuclear Polarization of Deuterated Molecules Enhanced by Cross-Polarization " J. Chem. Phys. **145**:
5   194203.

6   Leavesley, A., C. B. Wilson, M. Sherwin and S. Han (2018). "Effect of water/glycerol polymorphism
7   on dynamic nuclear polarization." Phys Chem Chem Phys **20** (15): 9897-9903.

8   Lipso, K. W., S. Bowen, O. Rybalko and J. H. Ardenkjaer-Larsen (2017). "Large dose hyperpolarized
9   water with dissolution-DNP at high magnetic field." J Magn Reson **274**: 65-72.

10   Liu, M. and C. Hilty (2018). "Metabolic Measurements of Nonpermeating Compounds in Live Cells
11   Using Hyperpolarized NMR." Anal Chem **90** (2): 1217-1222.

12   Malinowski, R. M., K. W. Lipso, M. H. Lerche and J. H. Ardenkjaer-Larsen (2016). "Dissolution
13   Dynamic Nuclear Polarization capability study with fluid path." J Magn Reson **272**: 141-146.

14   Milani, J., B. Vuichoud, A. Bornet, P. Mieville, R. Mottier, S. Jannin and G. Bodenhausen (2015). "A
15   magnetic tunnel to shelter hyperpolarized fluids." Review of Scientific Instruments **86** (2): 024101.

16   .Pinon, A. C., A. Capozzi and J. H. Ardenkjaer-Larsen (2020). "Hyperpolarization via dissolution
17   dynamic nuclear polarization: new technological and methodological advances." Communications
18   Chemistry **3**: 57.

19   Sadet, A., Emmanuelle M. M. Weber, A. Jhajharia, D. Kurzbach, G. Bodenhausen, E. Miclet and D.
20   Abergel (2018). "Kinetic rates of chemical metabolic processes determined by NMR boosted by
21   dissolution dynamic nuclear polarization." Chem. Eur. J. **24**: 5456 – 5461.

22   Szekely, O., G. L. Olsen, I. C. Felli and L. Frydman (2018). "High-resolution 2D NMR of disordered
23   proteins enhanced by hyperpolarized water." Anal Chem. **90**: 6169–6177.

24   Tayler, M. C., I. Marco-Rius, M. I. Kettunen, K. M. Brindle, M. H. Levitt and G. Pileio (2012). "Direct
25   enhancement of nuclear singlet order by dynamic nuclear polarization." J Am Chem Soc **134** (18): 7668-
26   7671.

27   Vuichoud, B., A. Bornet, F. d. Nanteuil, J. Milani, E. Canet, X. Ji, P. Miéville, E. Weber, D. Kurzbach,
28   A. Flamm, R. Konrat, A. D. Gossert, S. Jannin and G. Bodenhausen (2016). "Filterable Agents for
29   Hyperpolarization of Water, Metabolites, and Proteins." Chem. Eur. J. **22**: 14696-14700.

30   Vuichoud, B., J. Milani, Q. Chappuis, A. Bornet, G. Bodenhausen and S. Jannin (2015). "Measuring
31   absolute spin polarization in dissolution-DNP by Spin PolarimetrY Magnetic Resonance (SPY-MR)." J.
32   Magn. Reson. **260**: 127-135.

33   Wang, Y. and C. Hilty (2019). "Determination of Ligand Binding Epitope Structures Using
34   Polarization Transfer from Hyperpolarized Ligands." J Med Chem **62** (5): 2419-2427.

35   Weber, E. M. M., G. Sicoli, H. Vezin, G. Frébourg, D. Abergel, G. Bodenhausen and D. Kurzbach
36   (2018). "Sample Ripening through Nanophase Separation Influences the Performance of Dynamic
37   Nuclear Polarization." Angew. Chem. Int. Ed., **130**: 5267-5271.

38